Nonlinear Simulations of Toroidal Geometry RFPs with Sheared Flow

Carl Sovinec and James Reynolds
University of Wisconsin-Madison

American Physical Society, Division of Plasma Physics
43rd Annual Meeting

October 29-November 2, 2001

Long Beach, California

Objectives

1. To determine the influence of toroidal geometry on low-β reversed-field pinch configurations.

2. To explore the influence of sheared flow on mode structure and on nonlinear coupling in toroidal geometry.

Outline

I. Introduction
   A. Background
   B. Geometric considerations
   C. Modeling
II. Aspect ratio scans
   A. F-Θ
   B. Magnetic fluctuations
   C. Spectrum width
III. Laminar vs. single-helicity
   A. The role of viscosity
   B. Varying pinch parameter
IV. Initial results with sheared flow
   A. Enhanced momentum transport
   B. Magnetic fluctuations
V. Conclusions

Background

- Most numerical simulations and analytic computations for the RFP have been performed in periodic linear geometry.
- This is often a sound approximation:
  - Since $q<1$, pressure gradients cannot stabilize tearing modes (assuming p decreases with r). [Glasser, Greene, and Johnson, Phys. Fluids **18**, 875 (1975).]
  - Strong nonlinear coupling among resonant fluctuations of different poloidal index m is a characteristic of standard RFP operation. [Ho and Craddock, Phys. Fluids B **3**, 721 (1991).]
- A laminar version of the RFP dynamo, known as the "single-helicity state," exists at sufficient dissipation levels in periodic linear geometry. [Finn, Nebel, and Bathke, Phys. Fluids B **4**, 1262 (1992); Cappello and Escande, PRL **85**, 3838 (2000).]
  - The usual nonlinear coupling among different helicities is absent.
  - Toroidal geometry effects can make a qualitative difference in these conditions, due to linear coupling of different m.
- The stability of tearing modes may be influenced by flow shear.
  - Toroidal effects lead to a spectrum of m numbers in each mode.
  - Differential rotation of resonance surfaces affects the eigenvalue and spectral content of tearing modes.

Geometric Considerations

- Many low-order helicities are resonant in a typical RFP *q*-profile.

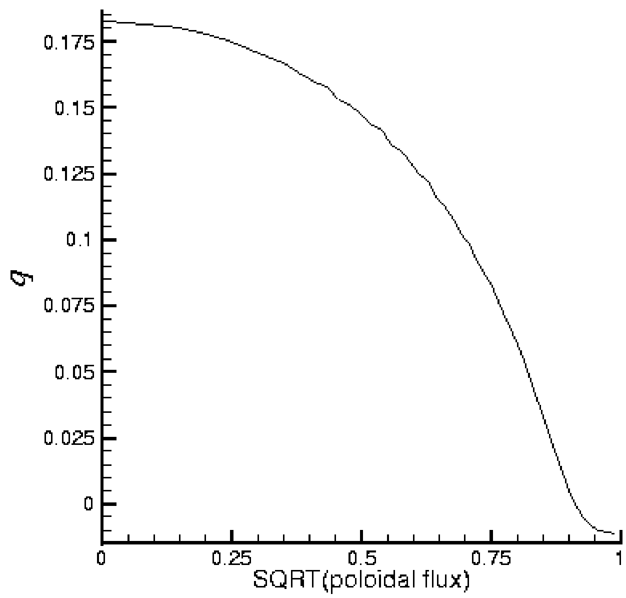

- The close spacing of the rational surfaces and the global nature of the dominant tearing modes allow for strong nonlinear coupling in standard operation.

- A well-established effect of toroidal geometry is that it leads to **linear** coupling among different helicities with the same *n*-value.

  - The gradient operator contains

$$\frac{1}{R}\frac{\partial}{\partial\varphi} = \frac{1}{(R_0 + r\cos(\theta))}\frac{\partial}{\partial\varphi}$$
$$= \frac{1}{R_0}\left(1 - \varepsilon\frac{r}{a}\cos(\theta) + \left(\varepsilon\frac{r}{a}\right)^2 \cos^2(\theta) - \ldots\right)\frac{\partial}{\partial\varphi}$$

  where $\varepsilon = a/R_0$ and the $\cos(\theta)$ terms lead to the coupling.

  - The poloidal asymmetry of the equilibrium (mainly the Shafranov shift) also leads to linear coupling.

- For an RFP *q*-profile we can expect the strongest poloidal coupling to occur between *m*=0 and *m*=1 helicities.

  - The unstable modes are predominantly $(m = 1, n \leq -2R/a)$ helicity resonant near *r*=0.

  - The corresponding (*m*=2, *n*) helicity is not resonant for these modes.

Modeling

To investigate the electromagnetic activity, we solve the resistive MHD equations in circular cross-section, toroidal and periodic linear geometries using the NIMROD simulation code, http://nimrodteam.org. Specifying $\beta \rightarrow 0$ for these studies:

$$\rho \frac{\partial \mathbf{V}}{\partial t} + \rho \mathbf{V} \cdot \nabla \mathbf{V} = \mathbf{J} \times \mathbf{B} + \nabla \cdot \left(\rho \nu \nabla \mathbf{V} \right)$$

$$\mathbf{E} = -\mathbf{V} \times \mathbf{B} + \eta \mathbf{J}$$

$$\frac{\partial \mathbf{B}}{\partial t} = -\nabla \times \mathbf{E}$$

- Density is uniform, though flow is not incompressible.
- Resistivity and viscosity are essentially uniform.
  [$1000 \leq \mathrm{S} \leq 25{,}000$ (mostly 2500 here) and
  $\mathrm{Pm} \equiv \mu_0 \nu / \eta = 1 - 100$]
- Voltage is dynamically adjusted to maintain the desired current. The time-scale for the feedback is comparable to the tearing time to avoid excitation of surface currents.
- Two-fluid effects may be important.
  - The drift ordering is more realistic for RFPs than the MHD ordering even at small β.
  - Worth further investigation.

- Numerical parameters:
  - Most of the simulations reported here have $0 \le n \le 42$.
  - Some of the simulations for laminar conditions have $0 \le n \le 21$; *R/a*=5 cases have $0 \le n \le 85$.
  - NIMROD uses finite elements to represent the poloidal plane. Simulations for the aspect ratio scan were run with a 48x48 or 64x64 (radial x azimuthal) mesh of bilinear finite elements.
  - When parameters are scanned to achieve laminar states, a 16x24 or 16x32 mesh of bicubic elements is used for a better representation of the magnetic field. [See "Nonlinear Fusion Magneto-Hydrodynamics with Finite Elements," Sherwood 2000, in http://nimrodteam.org/presentations.]

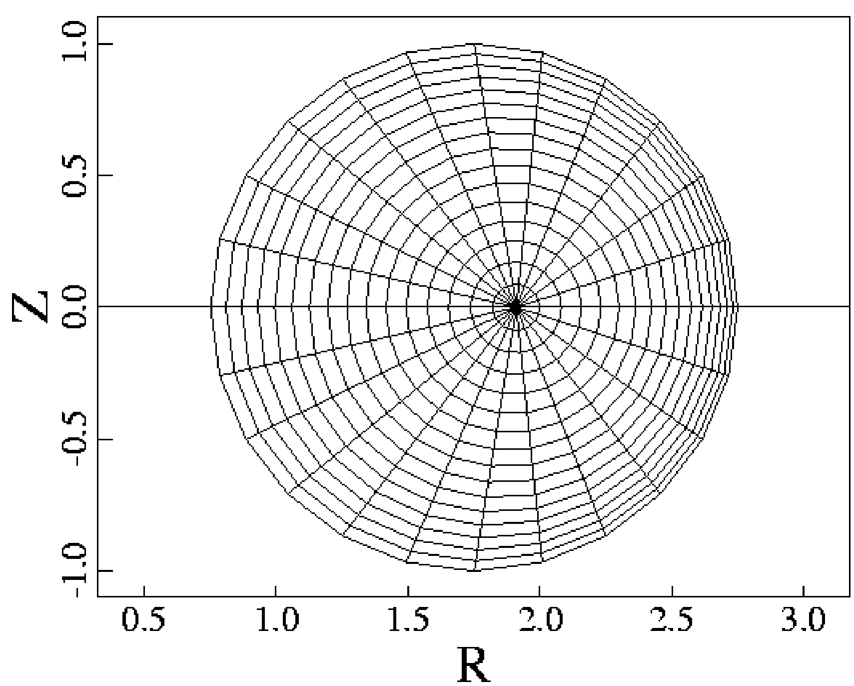

Aspect Ratio Scans in Toroidal and Periodic Linear Geometries

- Results on field reversal from dynamo action are similar in the two geometries, even at very low aspect ratio.

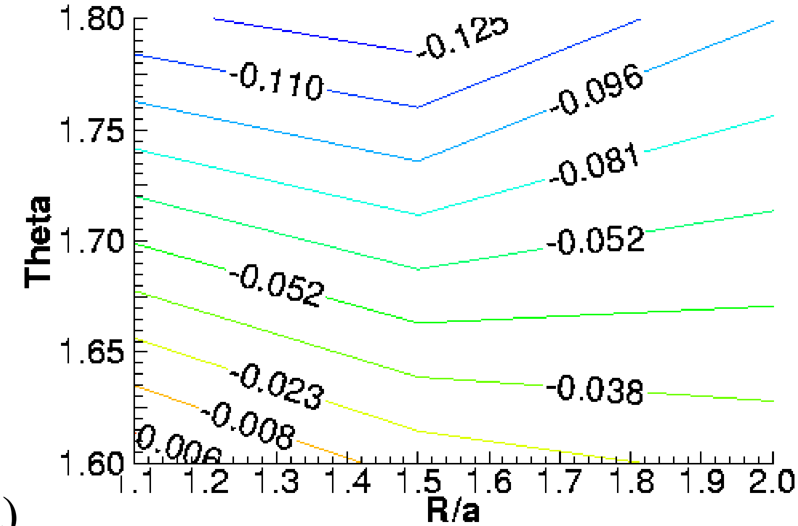

a)

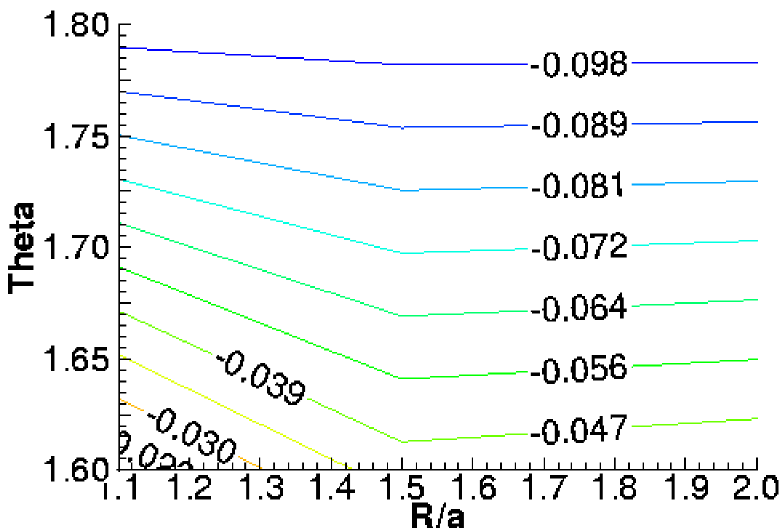

(b)

Comparison of time-averaged reversal parameter (*F*) resulting from simulations in (a) toroidal geometry and (b) periodic linear geometry at S=2500 and Pm=1.

- Magnetic fluctuation levels are also comparable.

geometry	*R/a*	Θ	$\frac{n > 0\,\text{energy}}{\text{total energy}}$
toroidal	1.1	1.6	0.091
linear	1.1	1.6	0.080
toroidal	1.1	1.8	0.16
linear	1.1	1.8	0.097
toroidal	1.5	1.6	0.083
linear	1.5	1.6	0.085
toroidal	1.5	1.8	0.14
linear	1.5	1.8	0.10
toroidal	2	1.6	0.084
linear	2	1.6	0.087
toroidal	2	1.8	0.10
linear	2	1.8	0.10

Results are averaged over 1-2 tenths of a global diffusion time.

- Magnetic energy spectra plotted vs. *n* and summed over *m* for the two geometries are often nearly indistinguishable for standard multi-helicity states.

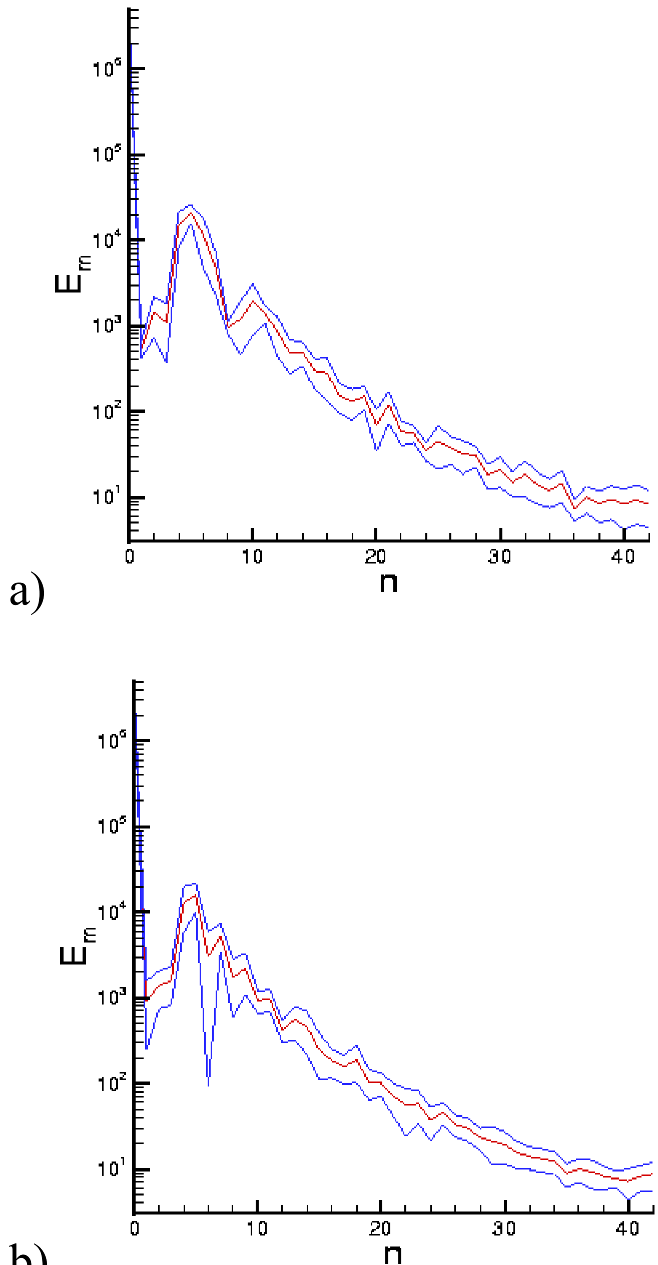

Magnetic fluctuation energy spectra for a) toroidal geometry and b) periodic linear geometry showing the temporal average (red) and ± one standard deviation (blue) for R/a=1.75, P_m=1, Θ=1.8.

- The spreading of the magnetic spectrum with *R/a* reported by Ho, *et al.* ["Effect of aspect ratio on magnetic field fluctuations in the reversed-field pinch," Phys. Plasmas **2**, 3407 (1995).], is also observed in toroidal geometry.

  - Each W_n is summed over m.
  - Nonlinear interaction seems to be more easily suppressed in toroidal geometry.

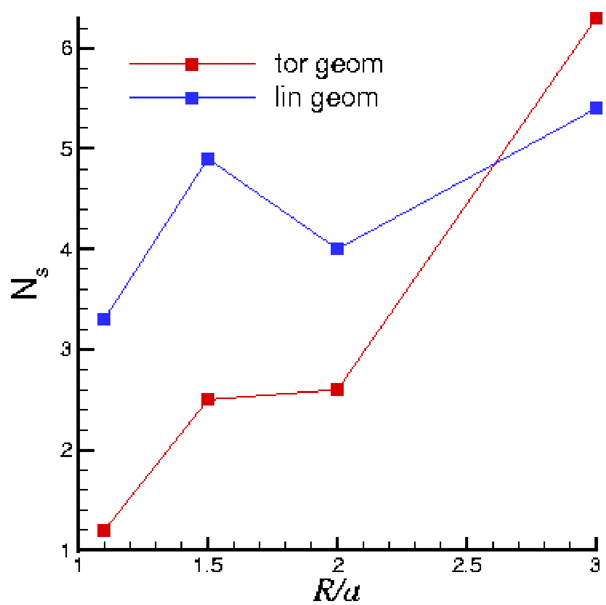

Simulation results on $N_s \equiv \left(\sum_n W_n \right)^2 \Big/ \sum_n W_n^2$ for Θ=1.6, P_m=1 simulations. At *R/a*=1.5, *q*(0) is slightly greater than 1/3.

Laminar RFP States

- As viscosity is increased there is a transition to steady or near-steady states.
- Cappello and Escande have established that this transition is more dependent on the Hartmann number ($\mathrm{H} \equiv \mathrm{S}\,\mathrm{Pm}^{-1/2}$) than the Lundquist number.

Transition to laminar states in periodic linear geometry with *R/a*=4. [Cappello and Escande, "Bifurcation in Viscoresistive MHD: The Hartmann Number and the Reversed Field Pinch," PRL **85**, 3838 (2000).]

- A transition to laminar behavior also occurs in toroidal geometry as Pm is increased. The following figure shows the transition in the toroidal *R/a*=1.75, Θ=1.8 case after Pm is increased from 1 to 10.

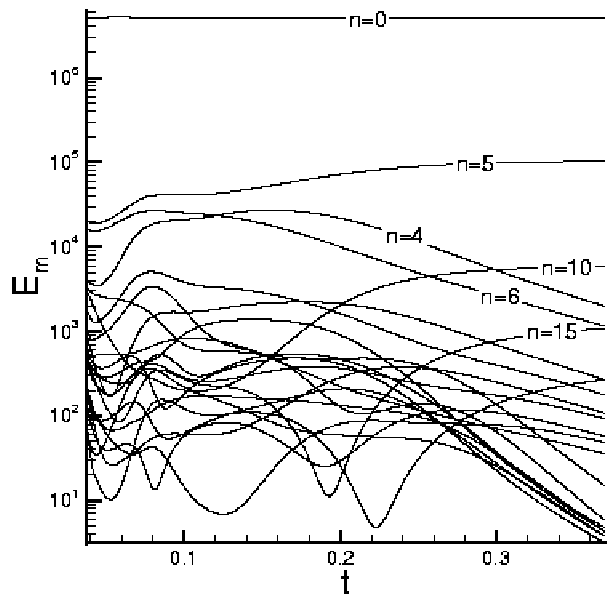

- Plotting energies vs. *n* (summed over *m*), the spectrum shows suppression of nonlinear coupling.

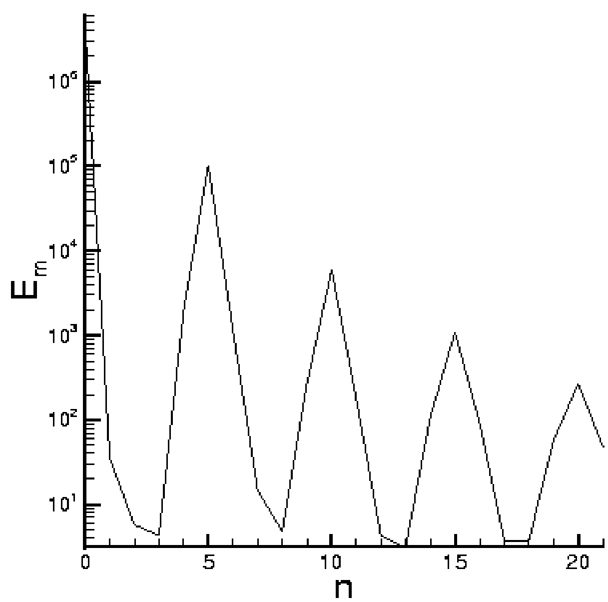

- Poincaré surfaces of section for **B** show that the final state is not single-helicity in toroidal geometry.

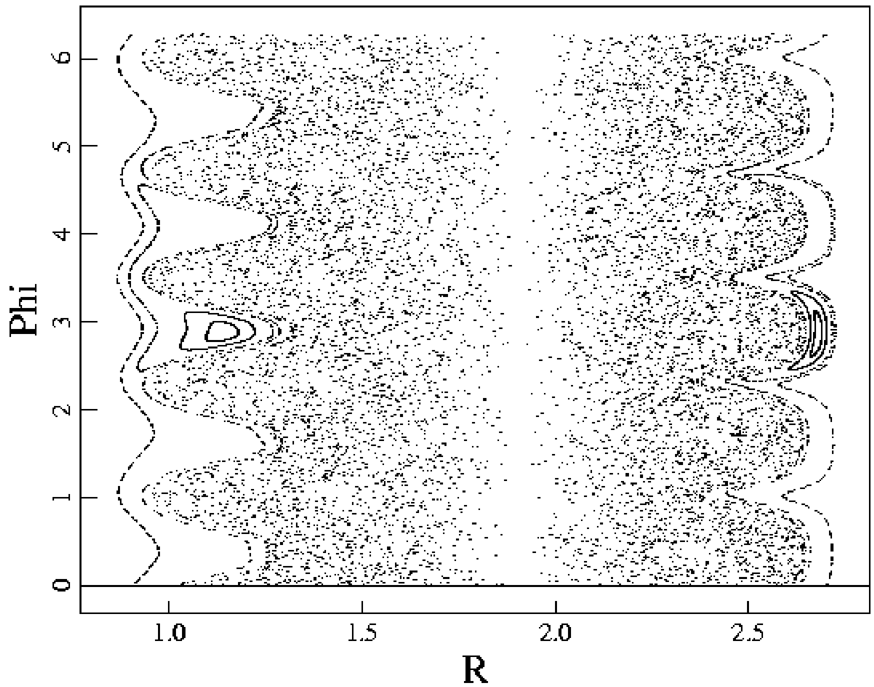

a)

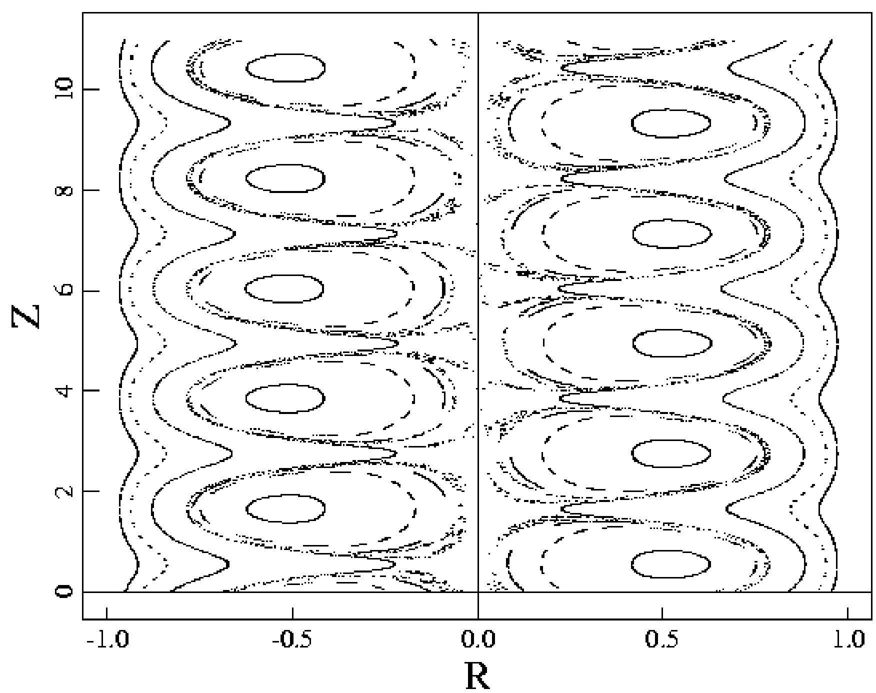

b)

Results from a) toroidal geometry and b) periodic linear geometry with Pm=10, *R/a*=1.75, Θ=1.8.

- The magnetic fluctuations in both configurations are dominated by the m/n=1/5 helicity, but the toroidal case has significant linear coupling among $m \pm 1$ about 1/5.

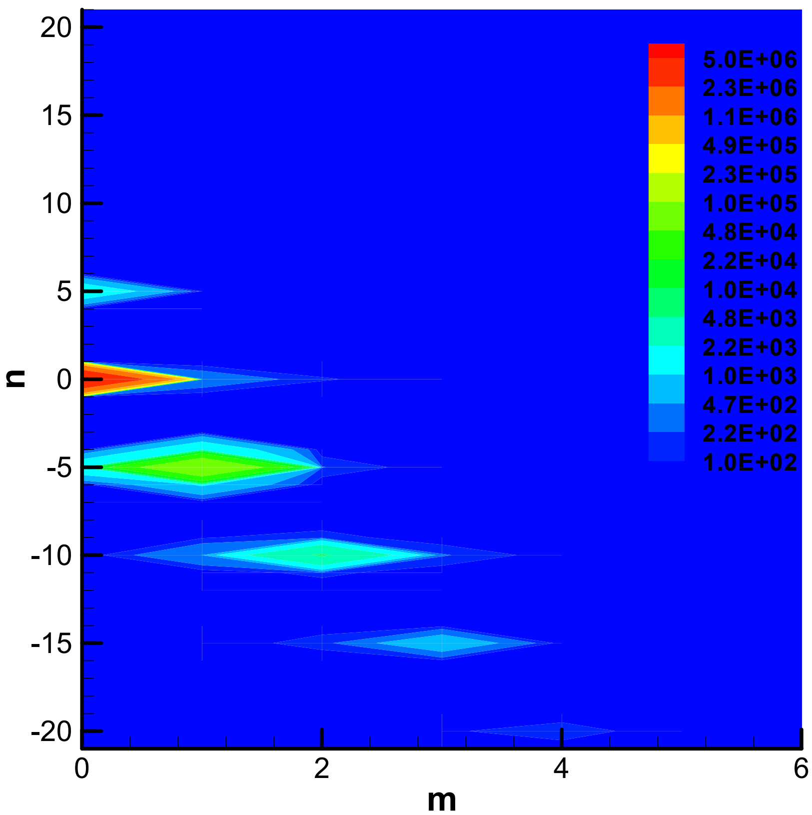

$E_{m,n} \equiv \iiint d\rho d\theta d\varphi \sum_j \left(\sqrt{g}\, B^j\right)_{m,n} \left(B_j\right)^*_{m,n} + c.c.$ for the toroidal simulation. The contra- and covariant components of **B** are defined in the straight field-line coordinates where φ is the toroidal symmetry angle. [diagnostic developed with Tom Gianakon, LANL].

- Increasing Pm to 100, the toroidal simulation loses reversal and a helical island chain forms in the interior.

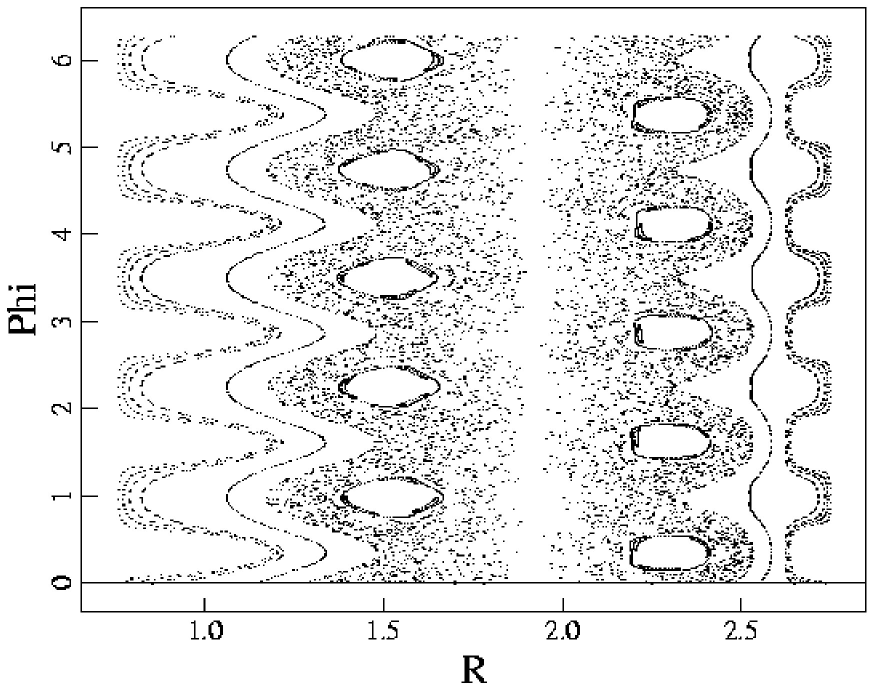

- In simulations with Pm=10, Θ=1.65, and *R/a*=1.75, the final state is steady, but not single helicity, even with linear geometry.

Linear Geometry Energies vs. Time

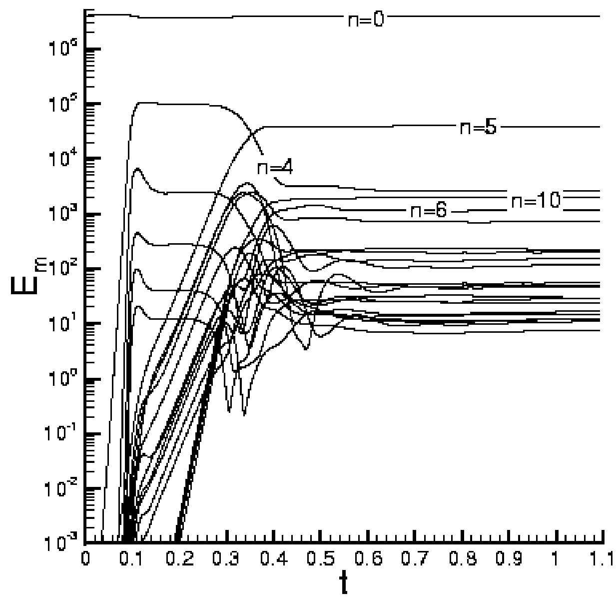

Linear Geom. Spectrum

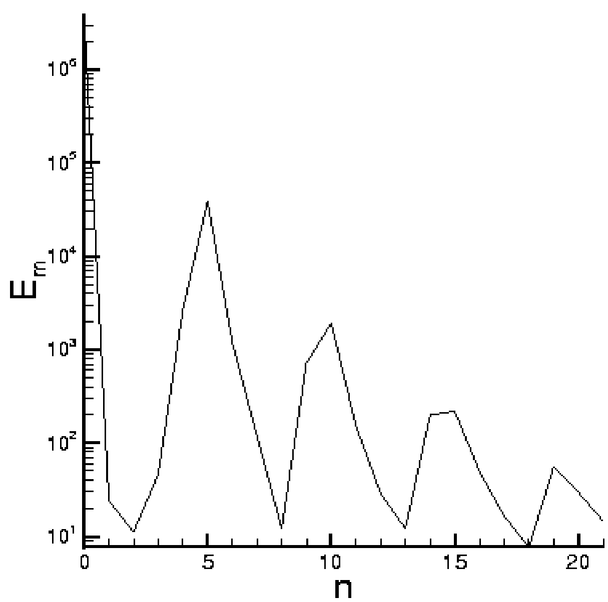

Toroidal Geom. Spectrum

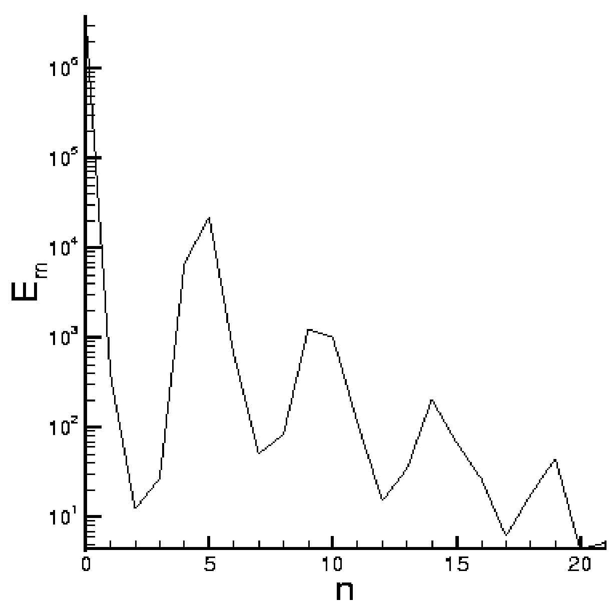

- These "quasi-single-helicity" states show small island structures [possibly by having one sufficiently *large* perturbation Escande, *et al.*, PRL **85**, 3169 (2000)].

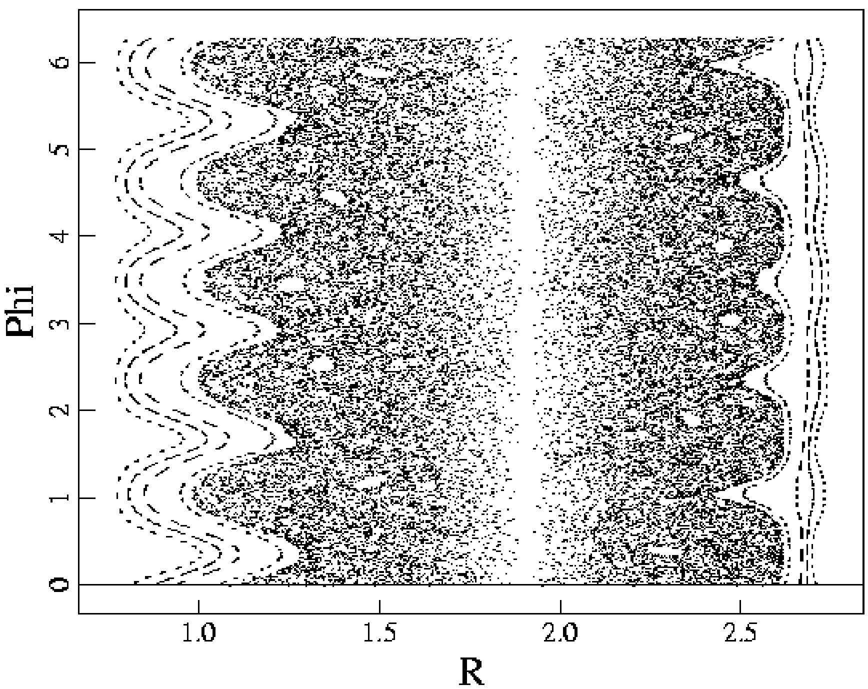

a)

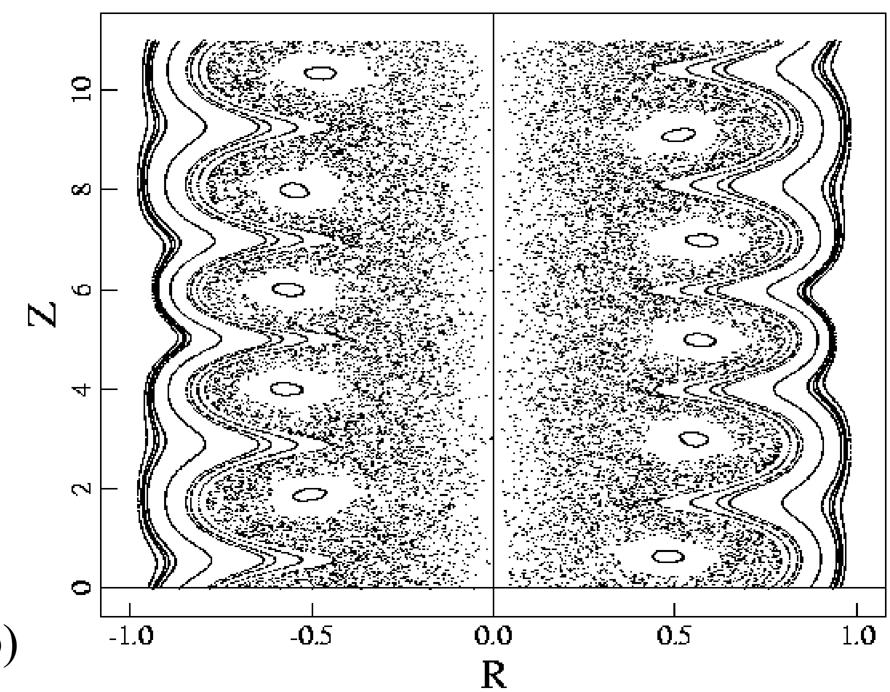

b)

QSH conditions in a) toroidal and b) periodic linear geometry.

- At lower current ($\Theta=1.4$), the pinch is not reversed, *m*=0 perturbations are not resonant, and the toroidal magnetic topology is qualitatively similar to the linear geometry result.

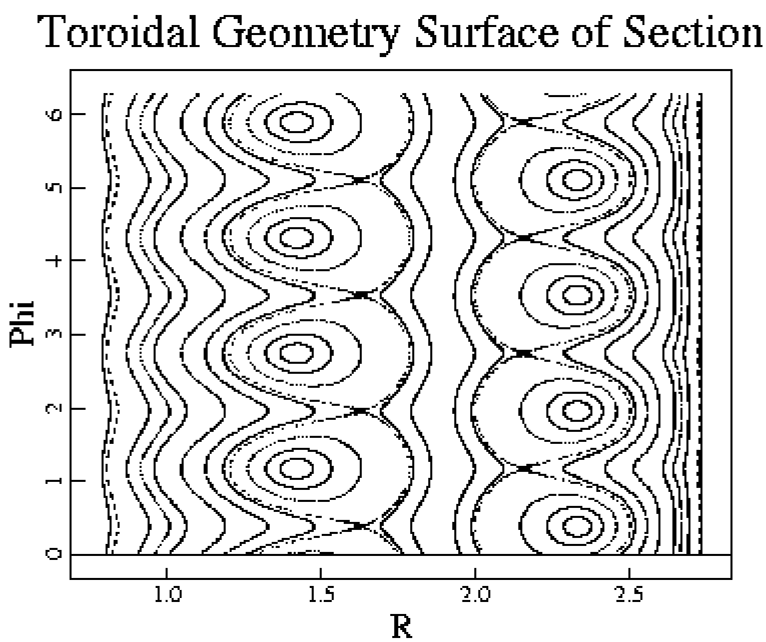

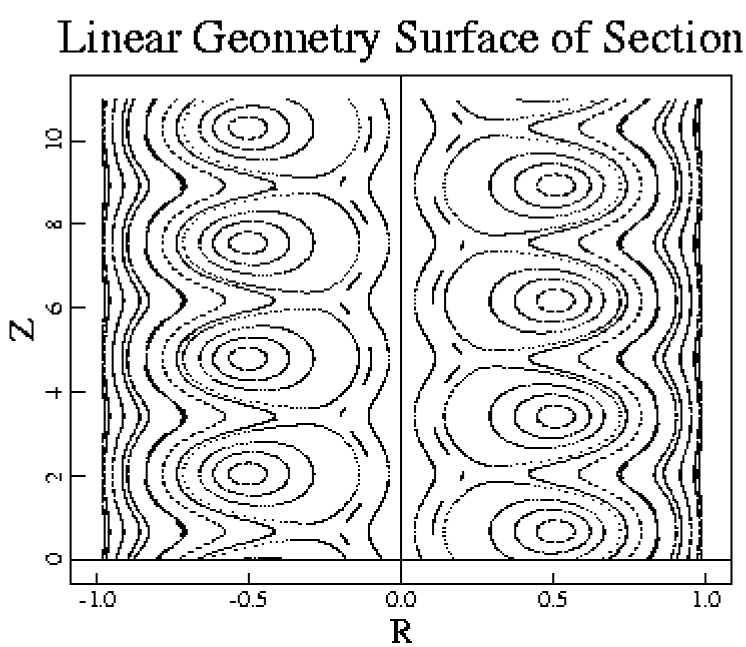

- The linear geometry results are influenced by the changing relative importance of the (1, -4) and (1, -5) modes, but single helicity occurs at both extremes (with or without reversal).

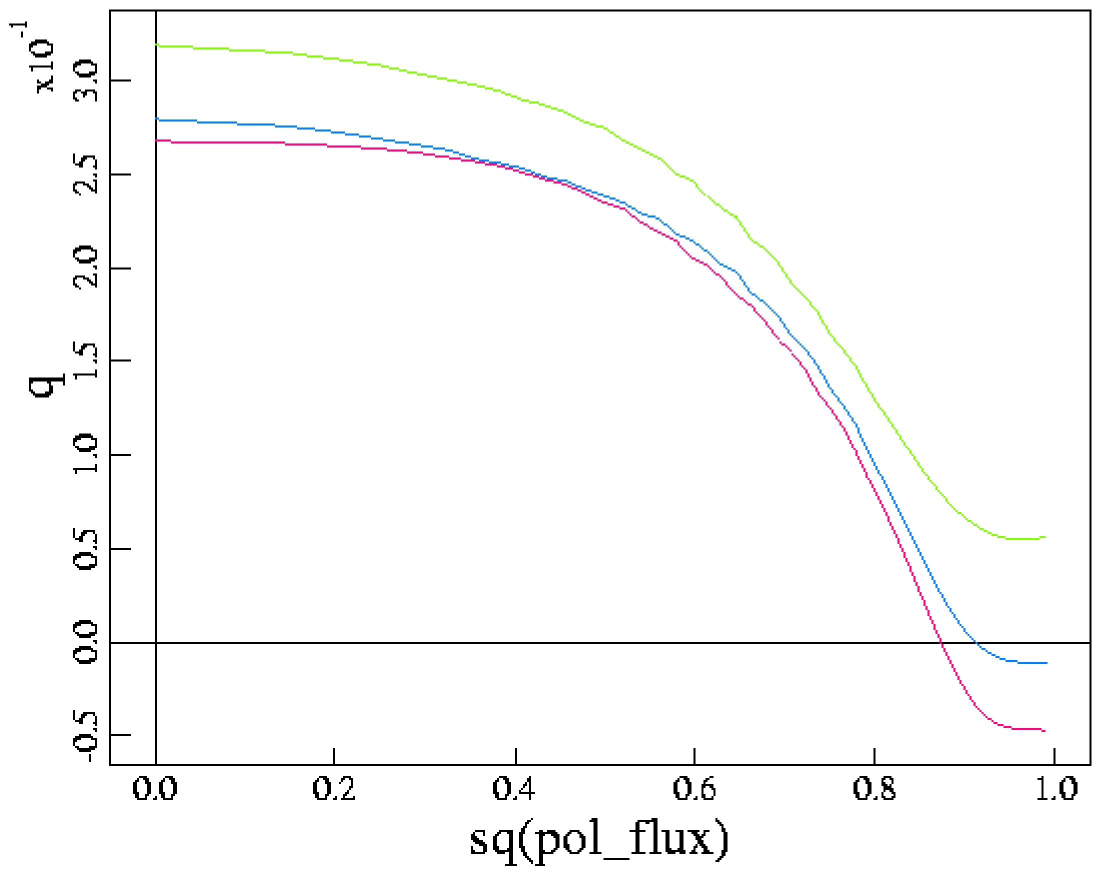

Safety factor (*q*) profiles for the linear geometry case as Θ is scanned from 1.4 (green line) to 1.8 (red line).

Like the results obtained by varying viscosity, the Θ-induced formation of flux surfaces in toroidal geometry is correlated with the loss of reversal, hence loss of resonance for m=0 fluctuations.

- At larger *R/a*, surfaces of section for the two geometries are also similar at $F > 0$.

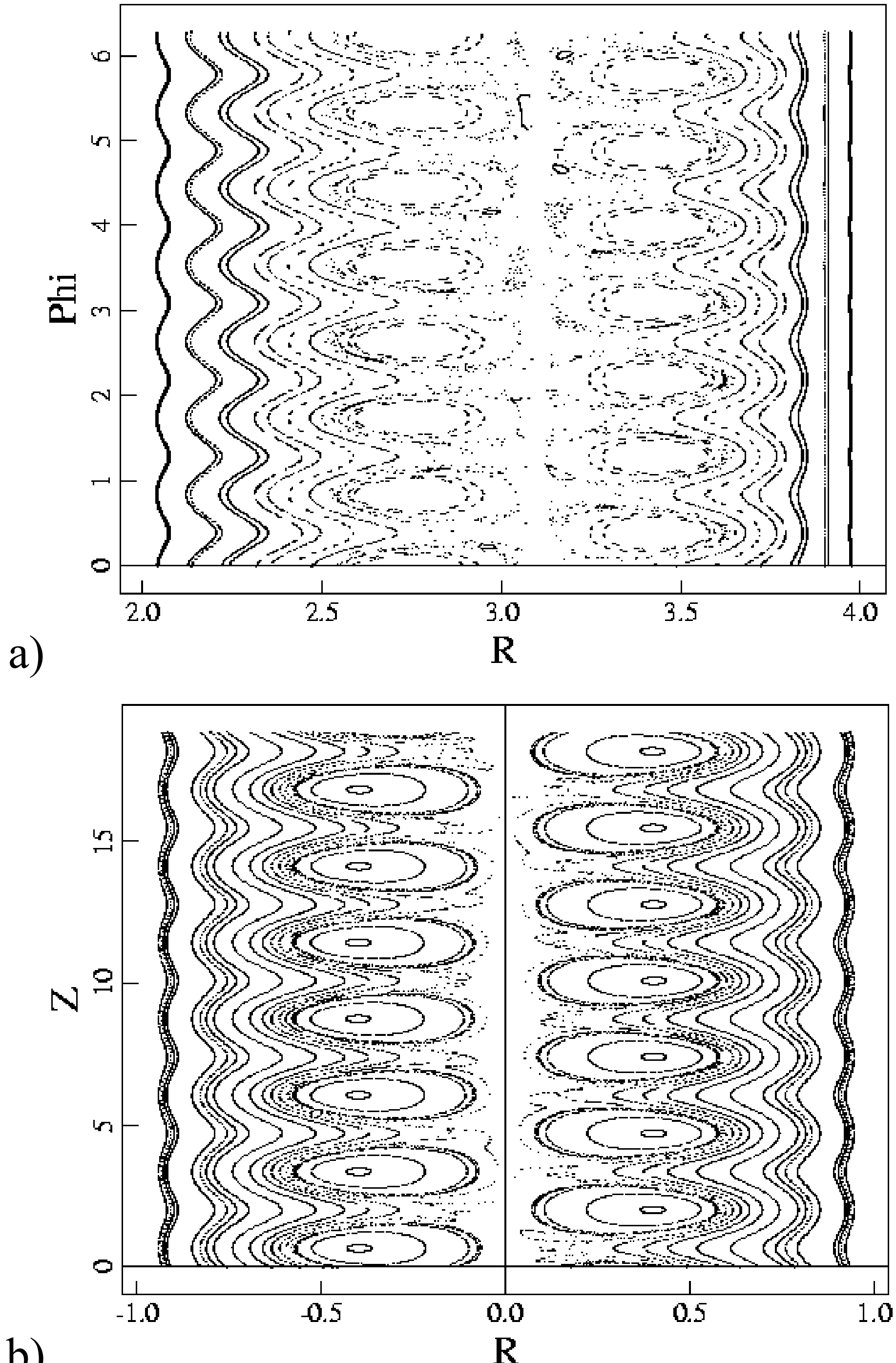

Results from a) toroidal geometry and b) periodic linear geometry with Pm=100, R/a=3, Θ=1.6.

Results with Sheared Flow

- Having established that toroidal geometry effects are strong enough to influence the topology of laminar states, we would like to determine if they could be used to improve confinement.
- Differential rotation of rational surfaces alters the linear properties of the resonant modes. If rotation reduces the growth rate of MHD instability, it may result in lower fluctuation amplitudes at saturation, if not complete stability.
- To investigate this possibility numerically, a $\hat{\varphi}$-directed momentum source $\propto R/R_0$ and no-slip boundary conditions are used to induce an approximately parabolic toroidal flow profile.
  - $$\rho\frac{\partial \mathbf{V}}{\partial t} + \rho\mathbf{V}\cdot\nabla\mathbf{V} = \mathbf{J}\times\mathbf{B} + \nabla\cdot\left(\rho\nu\nabla\mathbf{V}\right) + S_{\mathbf{p}}\frac{R}{R_0}\hat{\varphi}$$
  - The flow profile develops consistently with the toroidally symmetric part of **B**.

- Our RFP simulations are typically started from toroidally symmetric paramagnetic pinch solutions. With $S_{\mathbf{p}} a^2 / \rho \nu = 0.055 \, \mathrm{v_A}$, the linear growth rates are essentially the same as the no-flow growth rates.
  - The equilibrium is not reversed, so a dramatic change was not expected.
  - These growth rates may not reflect linear growth rates for equilibria with reversal.

Linear m=1 growth-rate comparison for a Θ=1.6, Pm=10 toroidally symmetric paramagnetic pinch. The momentum source has magnitude $0.055 \, \rho \nu \, \mathrm{v_A} / a^2$.

n	$\gamma \tau_A$ no flow	$\gamma \tau_A$ with flow
4	0.105	0.105
5	0.055	0.056
6	0.036	0.038
7	0.024	0.025

- The temporal evolution of kinetic energy in the $n > 0$ Fourier components differs little from the simulation without a momentum source.

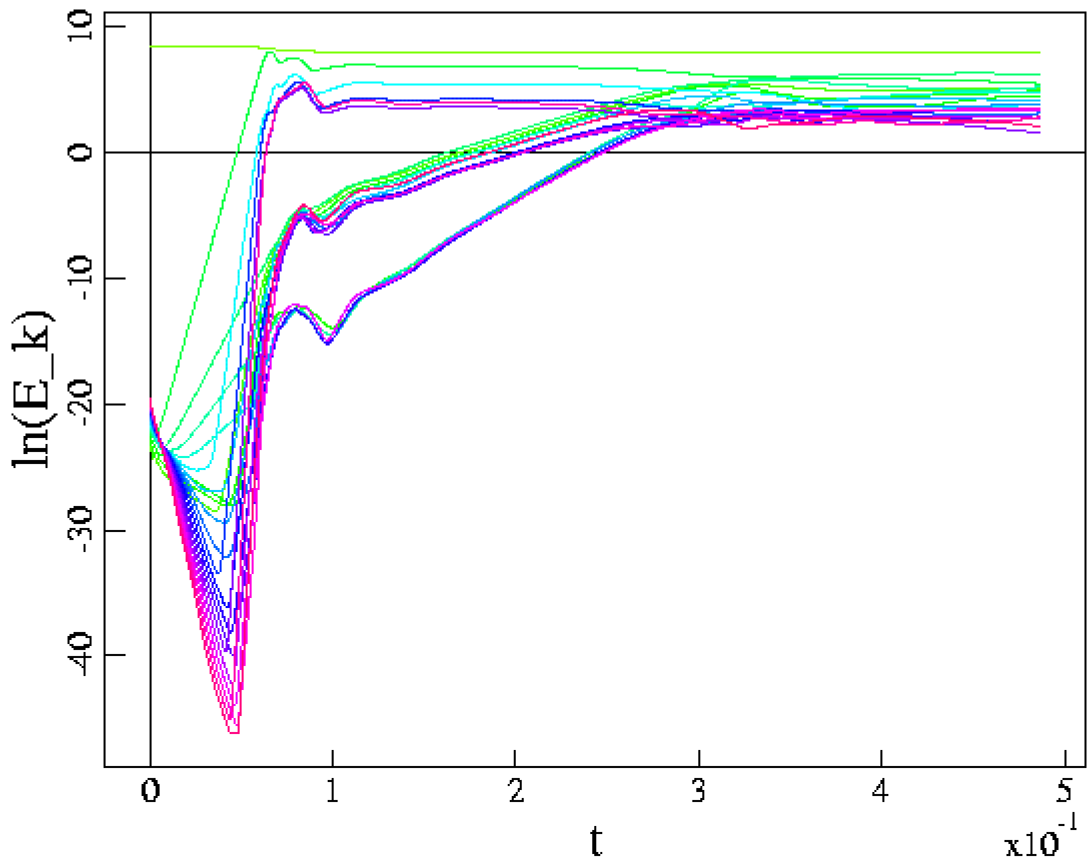

Natural logarithm of kinetic energy in each Fourier component as a function of time (in resistive diffusion times) starting with small perturbations from an unstable symmetric pinch.

- The n=0 component shows a significant decrease in kinetic energy as the fluctuations reach saturation. The presence of finite-amplitude fluctuations increases the rate of momentum transport to the wall.

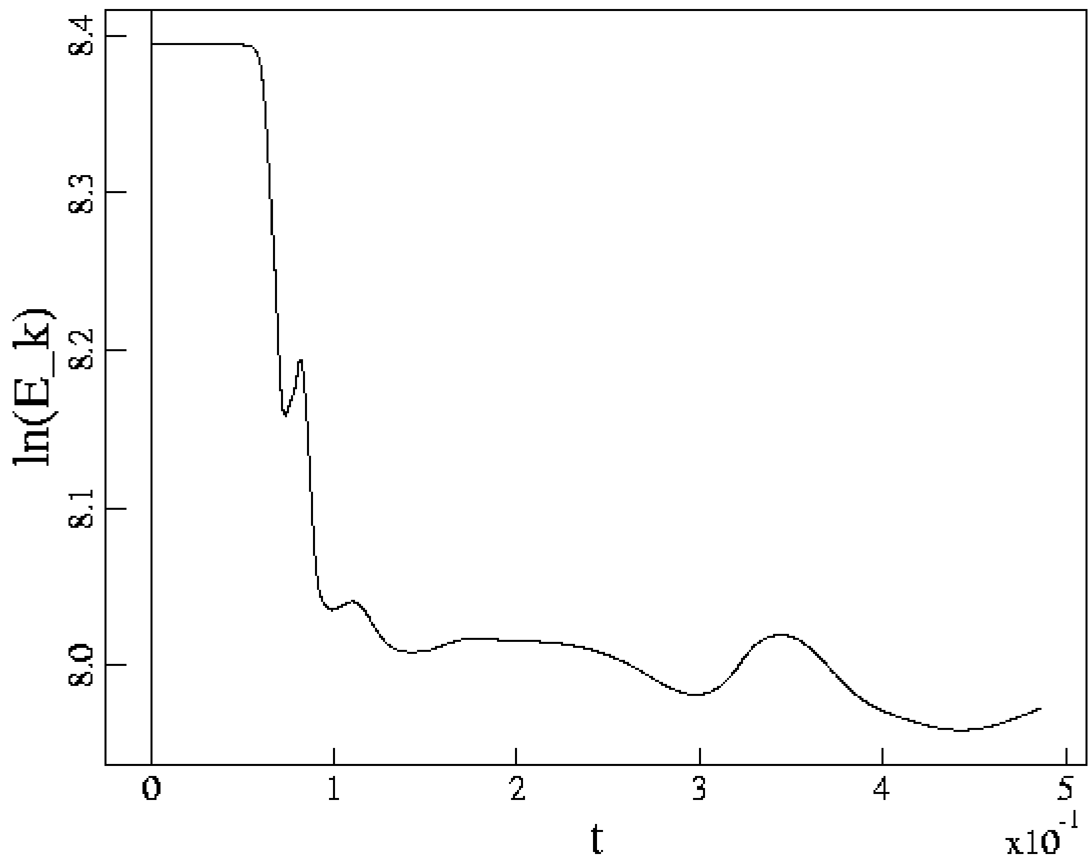

Natural logarithm of kinetic energy in the n=0 Fourier component as a function of time starting from a paramagnetic pinch with momentum source.

- The braking effect is also evident in the symmetric part of the toroidal flow profiles.

Contours of constant V_{φ} before saturation.

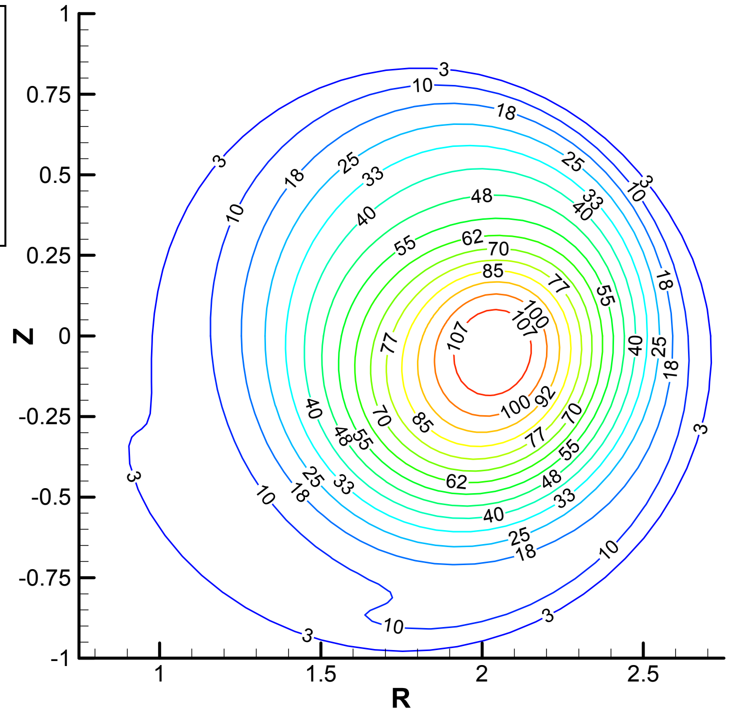

Contours of constant V_{φ} after saturation.

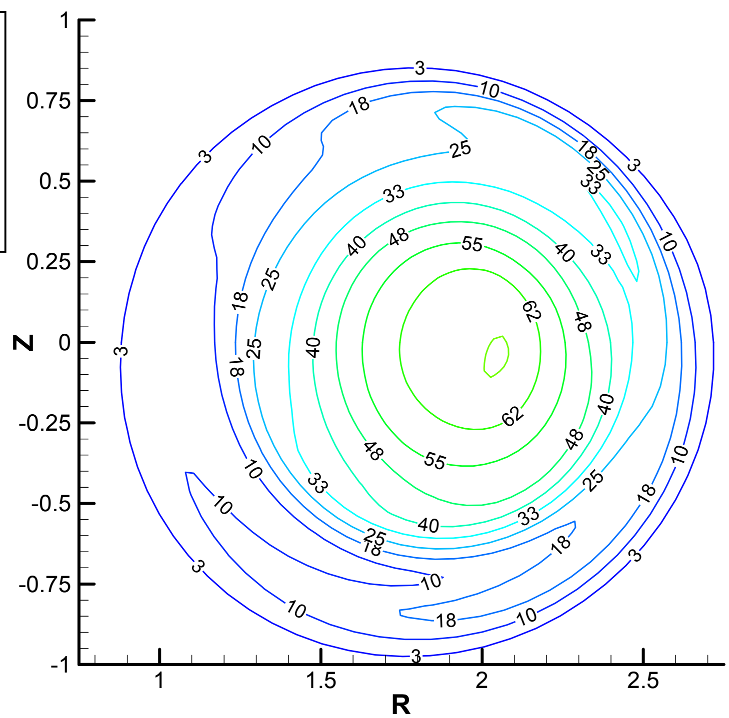

- A sequence of simulations explores the fluctuation levels resulting at three levels of momentum source magnitude.

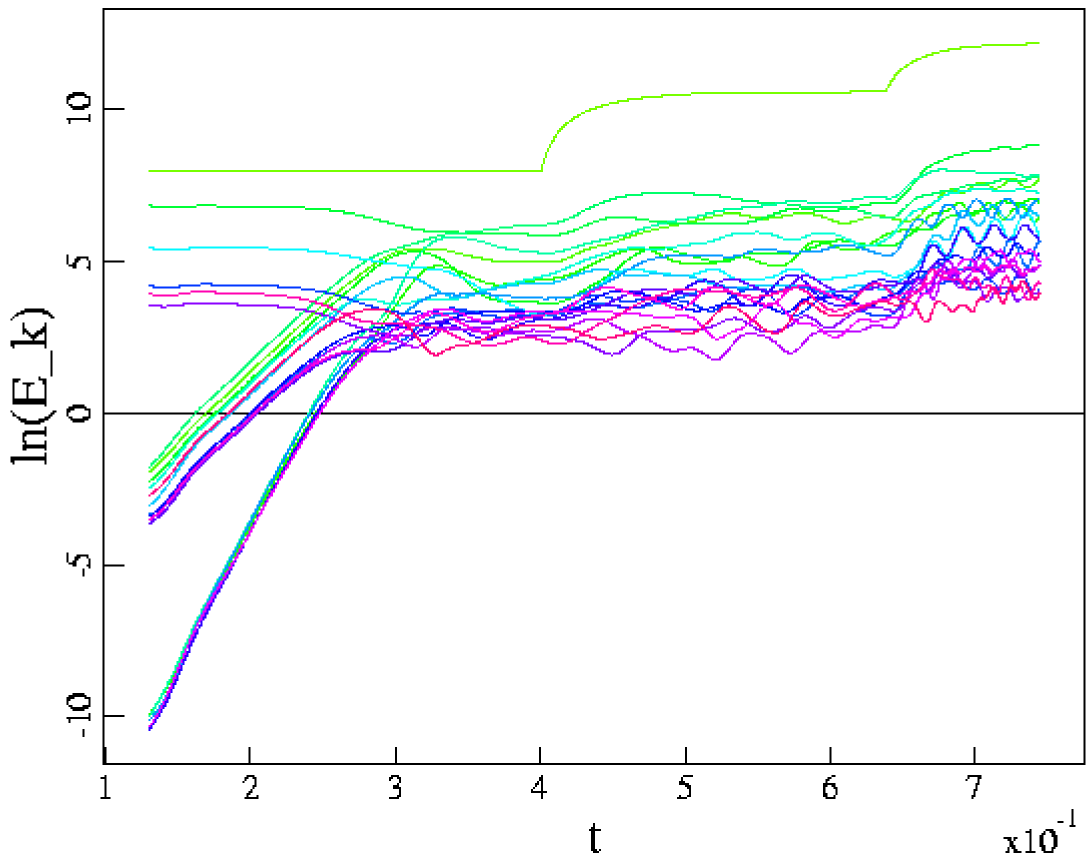

Natural logarithm of kinetic energy in each Fourier component

For t<0.4, $S_{\mathbf{p}} = 0.055\,\rho\nu\,\mathrm{v}_A / a^2$

For 0.4<t<0.64 $S_{\mathbf{p}} = 0.22\,\rho\nu\,\mathrm{v}_A / a^2$

For t>0.64 $S_{\mathbf{p}} = 0.55\,\rho\nu\,\mathrm{v}_A / a^2$

- The magnetic energy spectrum is only moderately affected by increasing the momentum source.

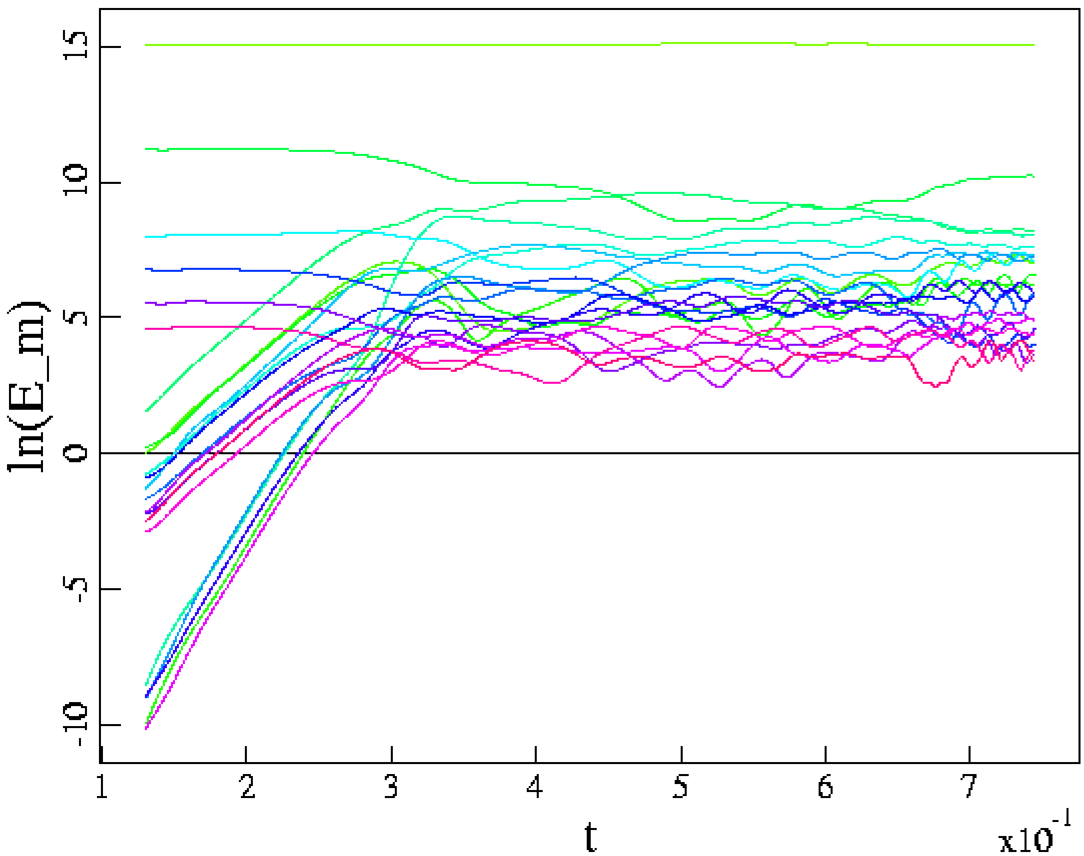

$S_{\mathbf{p}}$	rms $\tilde{b}/B_0$ (time-averaged)
0	0.10
$0.055\,\rho\nu\,\mathrm{v_A}/a^2$	0.11
$0.22\,\rho\nu\,\mathrm{v_A}/a^2$	0.92
$0.55\,\rho\nu\,\mathrm{v_A}/a^2$	0.11

- The flow distorts flux surfaces in the edge region; however, the magnetic topology remains stochastic in the core.

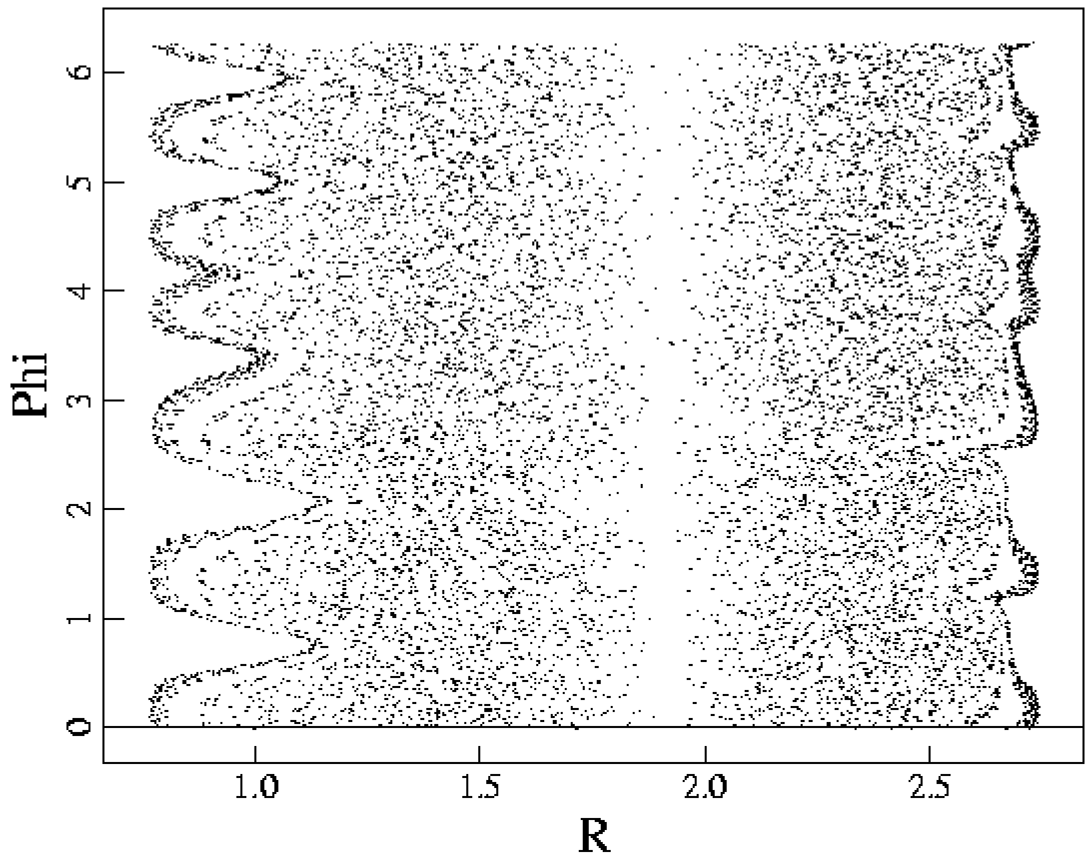

Conclusions

1. In typical multi-helicity RFP operation, toroidal geometry plays a minor role in comparison to nonlinear coupling.
2. In laminar conditions, toroidal geometry can make a qualitative difference. Conditions producing nonstochastic magnetic field in periodic linear geometry may have large regions of stochastic field in toroidal geometry.
3. All toroidal simulations showing laminar conditions with good flux surfaces are non-reversed states. The elimination of m=0 resonance seems to be essential.
4. Simulations with an imposed source of toroidal momentum exhibit enhanced momentum transport due to MHD fluctuations. A significant reduction of magnetic fluctuations has not been observed so far.

Acknowledgement

The authors wish to acknowledge the many important contributions of other members of the NIMROD Team.

This poster will be available through our web site, http://nimrodteam.org, shortly after the meeting.